Optimization of benzene removal by air gap membrane distillation using response surface methodology

Sara Pedram, Hamid Reza Mortaheb and Faranzaneh Arefi-Khonsa

ABSTRACT

An air gap membrane distillation (AGMD) system was applied for removal of benzene from benzene/water solution using polytetrafluoroethylene (PTFE) porous membrane. The experimental design using design methodology was applied for modeling and optimization of the process. The effects of air gap width and operation factors including feed temperature, concentration, flow rate, as well as their binary interactions on the permeation flux and separation factor were studied. Regression models, statistically validated by variance analysis, were developed to predict the AGMD performance. The optimum feed conditions for maximum separation were determined via D-optimal experimental design as temperature of 43 °C, concentration of 330 ppm, and flow rate of 3 mL/s at 5 mm air gap thickness.

Key words | air gap membrane distillation, benzene removal, D-optimal design, polytetrafluoroethylene (PTFE) membrane

Sara Pedram
Hamid Reza Mortaheb (corresponding author)
Petroleum Engineering Department,
Chemistry and Chemical Engineering Center of Iran,
P.O. Box 14335-186, Tehran,
Iran
E-mail: *mortaheb@ccerci.ac.ir*

Faranzaneh Arefi-Khonsa
Sorbonne Universités, UPMC Univ Paris 6, UMR8235, LISE,
4 Place Jussieu, 75252 Paris,
France

INTRODUCTION

Membrane distillation (MD) is one of the emerging thermally driven processes for desalination and wastewater treatment and known for more than 50 years. This process benefits from advantages such as its compactness, operability at low temperatures and pressures, and less fouling compared to conventional membrane processes such as reverse osmosis (AlHathal Al-Anezi *et al.* 2013). The process is specially significant for its capability to use alternative energy resources such as waste heats or solar and geothermal heat resources (Pangarkar & Deshmukh 2015). Purifying and concentrating chemicals (Alobaidani *et al.* 2008; Hwang *et al.* 2011; Summers & Lienhard 2013), food processing (Bandini & Sarti 2002; Bui *et al.* 2007), removal of heavy metals (Zolotarev *et al.* 1994), acid saline effluent (Gryta *et al.* 2006), ammonia, and volatile organic compounds (VOCs) (Couffin *et al.* 1998; Xie *et al.* 2009) from wastewater are among the applications of the MD process. The driving force in MD is associated with vapor pressure difference as well as temperature gradient across the two (feed/permeate) sides of a microporous hydrophobic membrane. The molecules of volatile component evaporate and migrate through the membrane pores to be condensed in the permeate side.

Air gap membrane distillation (AGMD) as one of the MD configurations, which was first introduced by Carlsson (1983), is characterized by a stagnant air gap inserted between the membrane and a condensation surface inside the permeate side of the membrane module. The feed solution is the only phase which is in direct contact with the membrane. The vapor molecules crossing the membrane pores traverse the air gap in the permeate side of the membrane and condense on the cold plate. The air gap provides low conductive heat loss through the membrane and higher thermal energy efficiency compared to direct contact MD. However, this space increases the mass transfer resistance and thus decreases the permeation flux. The air gap also

doi: 10.2166/aqua.2019.067

enables the process to be used for separation of volatile compounds from aqueous solutions (Khayet & Cojocaru 2012; AlHathal Al-Anezi *et al.* 2013).

Hydrophobicity is the important characteristic of the membranes applied in the MD process. The membranes often used in MD are commercially available and mostly fabricated from polytetrafluoroethylene (PTFE), polypropylene (PP), or polyvinylidene fluoride (PVDF) with porosities and pore sizes in the range of 0.6–0.95 and 0.2–1 μm, respectively (Camacho *et al.* 2013). Among these materials, PTFE membranes are of great interest because of their high hydrophobicity and proper mechanical and thermal stabilities.

He *et al.* (2011) carried out a comparative study on average pore size, density, porosity, liquid entry pressure (LEP), and contact angle (CA) of nine types of membranes. The results indicate that PTFE membrane is the most suitable one for the MD process due to its high porosity and hydrophobicity. The AGMD performance for desalination showed a higher permeation flux for the PTFE membrane than those for PVDF and PP membranes with a nearly complete salt rejection (He *et al.* 2011).

Alklaibi & Lior (2005) modeled the AGMD process by developing a two-dimensional model, in which a simultaneous numerical solution of momentum, energy, and diffusion equations of the feed and cold solutions was considered. It was concluded that the gap width has a significant effect on the AGMD performance, i.e., the permeation flux was enhanced 2.6-fold by five-fold decrease in the gap width. Moreover, it was found that the feed inlet temperature is the parameter to most affect the AGMD thermal efficiency, whereas the cooling temperature has much less effect.

Removal of water from nitric acid/water mixtures applying an AGMD system with hydrophobic PTFE membrane was studied by Matheswaran *et al.* (2007). The results showed a noteworthy decrease in the water selectivity and permeation flux by increasing the concentration of nitric acid in the feed solution up to the azeotropic concentration followed by an increase in the flux as a result of membrane wetting. Moreover, the flux and selectivity showed more sensitivity to the feed conditions than to the coolant liquid conditions. In a similar study, Alkhudhiri *et al.* (2013) applied three different PTFE membranes with the pore sizes of 0.2, 0.45, and 1 μm. The permeation flux was increased by increment of the pore size. The rejection factor increases for the membrane with 1 μm pore size while it was almost constant for the membranes with 0.2 and 0.45 μm pore sizes. The energy consumption was almost independent to variation in the membrane pore size.

Reviewing reported experimental AGMD studies revealed, that in most cases, to study the effect of operating parameters one independent parameter was varied while the other factors were kept at constant levels. Also, the interaction effects between the process parameters were ignored in this classical experimentation method. Over the past decade, the application of statistical experimental design in numerous experimental studies has been carried out successfully and seems to be helpful for investigations in MD processes. D-optimal experimental design that involves mathematical and statistical techniques for designing experiments (DOE) is considered as a promising method for further investigation on the interactions and optimization of the MD process. In this case, simultaneous optimization can be achieved by a limited number of experimental runs (Cojocaru & Zakrzewska-Trznadel 2007; Khayet *et al.* 2007, 2010a, 2010b; Khayet & Cojocaru 2012).

Benzene is considered as a major aromatic pollutant in industrial wastewater as well as in municipal water. Based on the regulations by the World Health Organization and some local organizations such as the US EPA, there are tight restrictions for the allowable concentration of benzene in drinking water. Because of limited solubility of benzene in water and therefore high energy requirements to apply conventional processes, such as distillation for the removal of benzene from water in such low concentrations, those processes are economically unfeasible for the separation of benzene from water. This would be one of the interesting areas to show the effective performance of the MD process.

In the present research, the effects of AGMD process parameters, i.e., feed temperature, feed concentration, and feed flow rate, on the performance of flat-sheet PTFE membranes are investigated for removal of benzene from water at two different air gaps. The statistical experimental design is applied for optimization of the AGMD process by prediction of permeation fluxes and separation factors.

EXPERIMENTAL

Air gap membrane distillation experiments

AGMD experiments are conducted using a laboratory setup illustrated schematically in Figure 1. The applied setup is composed of two cylindrical chambers for circulation of the feed and cooling liquid. The feed chamber is connected to the feed vessel for continuous circulation of the feed using a calibrated peristaltic pump (model 701520 – Cole-Parmer). A thermometer is inserted in the isolated opening of the feed chamber that controls the temperature of the feed chamber as the feed vessel is heated by a paraffin bath. The other chamber is connected to a circulator bath (Julabo, FP 50) to cool down the circulating water (set point = 10 °C). The diffused vapor is condensed by contact with a cooling plate, which is separated from the membrane by an air gap. The air gap width is adjusted by changing the thickness of Teflon frames inserted between the cold plate and the membrane. A commercial porous PTFE membrane (Sartorius Stedim Biotech) with an effective area of 10.8 cm^2 is applied. The specifications of the membrane are as follows: thickness = 80 µm, mean pore size = 0.45 µm, and porosity = 85%. The running time for each experiment is 6 h.

The permeation flux is calculated by:

$$J = \frac{v \times \rho}{S.t} \tag{1}$$

where J, v, ρ, S, and t represent permeation flux (kg/m^2.h), amount of permeate (m^3), water density (kg/m^3), membrane surface area in contact with the feed (m^2), and the time duration (h), respectively.

The separation factor of benzene is determined using the following equation:

$$\beta = \frac{y_B/(1-y_B)}{x_B/(1-x_B)} = \frac{y_B/x_B}{(1-y_B)/(1-x_B)} \tag{2}$$

where y_B and x_B represent the mole fractions of benzene in the permeate and feed, respectively.

The absorption UV–Vis spectroscopy (Perkin-Elmer Lambda 15 UV/VIS spectrophotometer) is applied to analyze the concentration of benzene in the AGMD process (wavelength of 254 nm).

The effects of feed temperature, concentration, and flow rate as well as the air gap width on the performance are investigated while the cold side temperature and recycling volumetric rate are kept constant at 10 °C and 20 mL/s, respectively.

Experimental design

Response surface methodology (RSM) is applied as a mathematical and statistical method for response prediction and optimization. Design of experiments (DOE) can provide the relationship between several inputs and one or more response variables (Carlsson 1983). Central composite

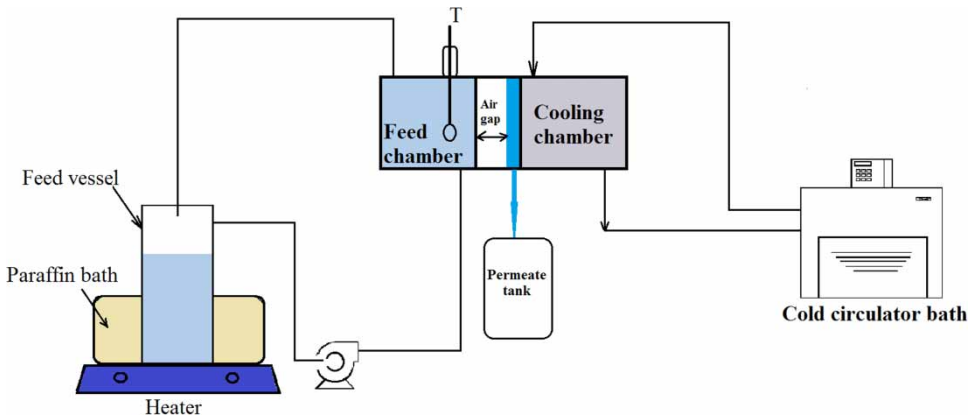

Figure 1 | Schematic diagram of experimental AGMD setup.

design (CCD) as the DOE approach and factorial design (FD) are preferred because of reliable model precision. However, some limitations in the design space may restrict the application of the method. In addition, it requires a large number of experiments.

Most of the common methods of experimental designs (CCD, Box–Behnken, and full FD) are not appropriate for some cases such as certain treatments (combinations of factor levels), or when the experimental zone is defined irregularly. In order to overcome such limitations, D-optimal design is considered as a useful alternative second-order model, which requires fewer experiments and can handle a mixed number of levels with reliable predictions. Therefore, it is possible to design the experiments having one quantitative factor with two levels and two qualitative factors having three levels each.

In this study, the D-optimal design with three factors, i.e., feed temperature, feed initial concentration, and feed flow rate at three levels and one other factor, air gap width, at two levels was employed. An empirical second-order polynomial model is selected for predicting and optimizing the model. The general form of such a polynomial is written as:

$$y = a_0 + \sum_{i=1}^{k} a_i x_i + \sum_{i=1}^{k} a_{ii} x_i^2 + \sum_{i<j}^{k} a_{ij} x_i x_j + \varepsilon \quad (3)$$

where y denotes the predicted response, a_0 is a constant, a_i is the ith linear coefficient, a_{ii} is the ith quadratic coefficient, a_{ij} is the ith interaction coefficient, z_i is the independent variable, and ε is the statistical error (Montgomery 2001; Lazic 2004). The operating variables and their ranges are shown in Table 1. The factor levels are selected based on practical considerations. The output responses are permeation flux (J) and separation factor (β).

Table 1 | Actual values of experimental variables used for AGMD experimental design

Independent variable	Coded variables	Low level	High level
Feed temperature, T_f (°C)	A	33	56
Initial feed concentration, C_0 (ppm)	B	120	330
Feed flow rate, F_f (mL/s)	C	1.6	3.4
Air gap width (mm)	D	3	5

RESULTS AND DISCUSSION

The effects of individual and interaction between the independent variables on the permeate flux and separation factor were determined by RSM. Experiments were performed randomly in order to reduce the effects of uncontrolled factors or noises. Table 2 shows the D-optimal experimental plan in terms of actual factor values and the corresponding results.

Data analysis

On the basis of D-optimal design and the recorded responses summarized in Table 2, the following quadratic equations in terms of coded variables are developed for the permeation flux (J) and separation factor (β):

$$J = 2.42 + 0.70\mathrm{A} + 0.19\mathrm{B} + 0.10\mathrm{C} - 0.88\mathrm{D} - 1.13\mathrm{AD} - 1.16\mathrm{C}^2 \quad (4)$$

$$\beta = 15.23 - 0.64\mathrm{A} + 0.75\mathrm{B} + 0.38\mathrm{C} + 1.49\mathrm{D} + 0.29\mathrm{BD} - 1.02\mathrm{A}^2 - 0.52\mathrm{C}^2 \quad (5)$$

In order to investigate the significances of developed second-order models and their coefficients, the analysis of variance (ANOVA) is applied. The results of ANOVA tests are shown in Table 3. The statistical significance of the regression models is determined in terms of F-value and P-value. The mathematical relationships used for computation of statistical estimators (i.e., F-value, R^2, R^2_{adj}) can be found elsewhere (Montgomery 2001; Lazic 2004). As seen in Table 3, the low P-values for J and β (less than 0.0001) imply that the models are significant. In order to enhance the regression quality, terms with high P-values (greater than 0.100) are removed manually. The R^2 value, as a measure of variation around the mean, should be rather high to ensure a satisfactory adjustment of regression model to the experimental data. The R^2 values for flux and separation

Table 2 | D-optimal experimental runs and corresponding responses

	Factors (input variables)				Responses	
Run number	Feed temperature A (°C)	Initial feed concentration B (ppm)	Feed flow rate C (mL/s)	Air gap width D (mm)	Flux J (kg/m^2 h)	Separation factor β (%)
1	45	120	1.6	5	1.23	14.6
2	33	225	3.4	3	2.31	13.4
3	45	120	3.4	5	1.25	15.7
4	45	330	1.6	5	1.25	16.8
5	56	330	2.5	3	4.38	13.4
6	33	225	1.6	3	2.14	12.7
7	45	330	3.4	5	1.63	17.5
8	45	225	2.5	3	3.36	13.2
9	56	225	1.6	5	1.63	14.4
10	56	225	1.6	3	3.86	10.4
11	45	330	1.6	5	1.48	16.3
12	45	120	3.4	5	1.27	15.3
13	33	120	2.5	3	2.2	12.8
14	33	330	2.5	3	2.66	13.8
15	45	330	3.4	5	1.76	17.9
16	56	120	2.5	3	3.64	11.3
17	56	225	2.5	5	2.39	15.3
18	56	225	3.4	3	4.24	11.7
19	45	225	2.5	3	3.17	13.3
20	33	330	2.5	3	2.81	13.1
21	33	120	2.5	5	0.77	15.1
22	45	120	1.6	3	3.18	13.0
23	33	225	2.5	5	0.99	16.5
24	33	225	1.6	5	0.78	15.8

factor are found to be 0.9819 and 0.9572, indicating that more than 98% and 0.95% of variability in the response can be explained by the model. Furthermore, the predicted R-squared values are in reasonable agreement with the adjusted R-squared values (within 0.2) for both models. The ANOVA results indicate that the developed empirical models are valid in terms of statistical point of view.

The surface response models (Equations (4) and (5)) applied to predict the permeation flux and separation factor at different values of feed temperature, flow rate, feed initial concentration, and air gap widths are in good agreement with the experimental values, as represented in Figure 2. The adequacy of the model is then confirmed for the predictions and optimization considering the statistical tests.

Effect of operating parameters on permeate flux

The perturbation plots are applied for comparing the effects of all factors at a particular point in the design space. The plots for permeation flux are shown in Figure 3. The responses are depicted by changing one factor over its range while keeping the other factors constant. These effects are demonstrated at the midpoint of the design space (temperature: 45°, feed concentration: 225 ppm, and feed flow rate: 2.5 mL/s) for both air gap thicknesses of 3 and 5 mm. The steep slope of temperature illustrates the sensitivity of

Table 3 | Analysis of variance (ANOVA) for permeation flux and separation factor

Source	Sum of squares	DF	Mean square	*F* value	*P*-value prob > F
Response: J					
Model	27.51	6	4.59	153.88	<0.0001
Residual	0.51	17	0.030		
Lack of fit	2.790.44	12	0.037	2.86	0.1271
Pure error	0.880.064	5	0.013		
$R^2 = 0.9819$, $R^2_{adj} = 0.9755$, $R^2_{pre} = 0.9583$, Adequate precision = 38.779					
Response: β					
Model	82.05	7	11.72	51.09	<0.0001
Residual	3.67	16	0.23		
Lack of fit	2.79	11	0.25	1.44	0.3629
Pure error	0.88	5	0.18		
$R^2 = 0.9572$, $R^2_{adj} = 0.9384$, $R^2_{pre} = 0.9014$, Adequate precision = 23.247					

this factor, as also can be concluded from Equation (4). The comparatively flat line for the feed flow rate shows its lesser impact on the permeation flux as is implied also from low coefficients of the corresponding factor in Equation (4). Similar results are reported elsewhere (Hou *et al.* 2012; Razmjou *et al.* 2012).

The effects of factors upon the response (permeate flux) were studied using three dimensional plots. Figure 4 shows the effect of feed temperature (T_f), feed flow rate (F_f), and concentration (C_0) on the permeation flux (J) for both 3 and 5 mm air gaps. Increasing the feed flow rate causes a slight increase in the permeate flux. This is attributed to the increase in mass transfer coefficient due to decline in temperature and concentration polarizations at the feed side interface. On the other hand, increasing the feed temperature leads to an increase in the permeation flux due to exponential variation of the feed vapor pressure as the driving force based on the Antoine equation. The plot reveals that the effect of temperature is more pronounced compared to that of the flow rate. In addition, the permeation flux is increased by increasing the benzene concentration in the feed. This is attributed to increase in the partial and total vapor pressures by increasing the concentration of volatile component considering Henry's law for dilute solutions. However, the effect of concentration is insignificant as a limited range of concentration is considered in this study.

The main purpose of applying an air gap in the MD process is to reduce the conductive heat loss between the membrane and the cold surface. As the air gap width increases, the conductive heat transfer in the air gap will decrease, however, it causes a higher mass transfer resistance between the membrane and the condensing surface. Therefore, a smaller amount of permeation flux is expected at a larger distance. The mean fall in the permeation flux is more than 50% by increasing the air gap thickness from 3 to 5 mm in the present study. Moreover, Figure 5 reveals that

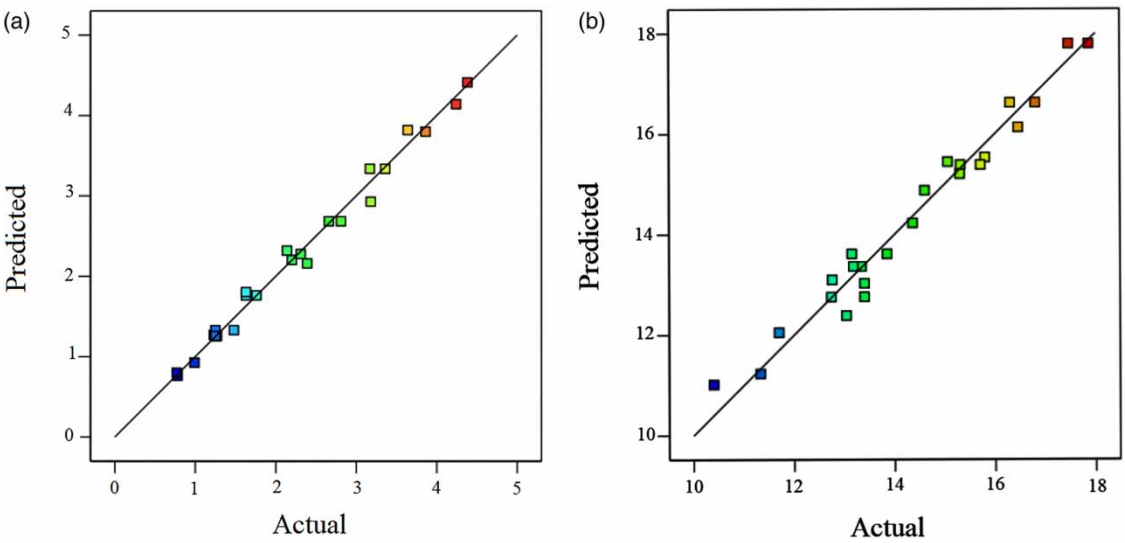

Figure 2 | Plots of predicted versus actual values for (a) permeation flux and (b) separation factor.

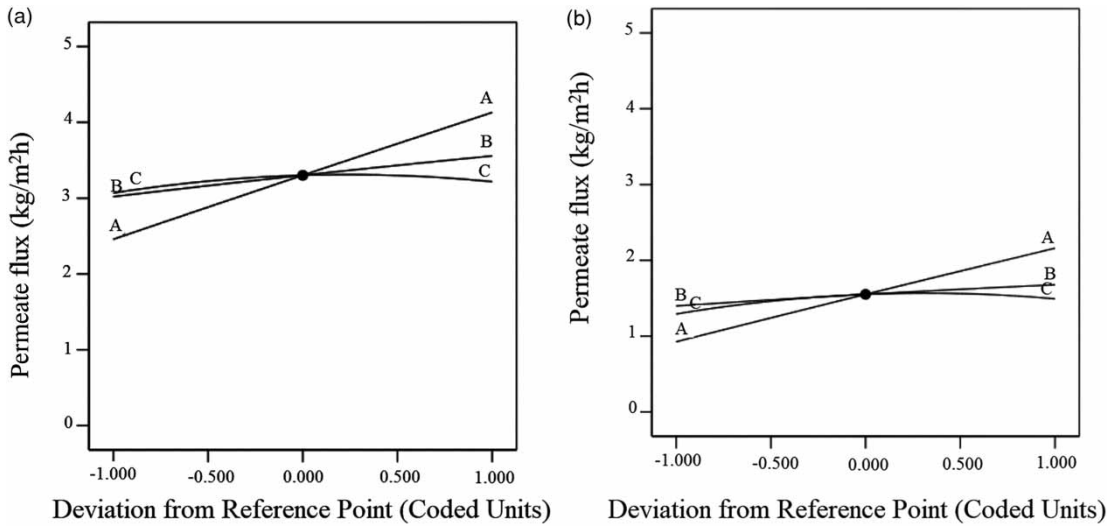

Figure 3 | Perturbation plots for permeation flux in (a) $\delta = 3$ mm and (b) $\delta = 5$ mm ((A) temperature, (B) concentration, and (C) feed flow rate).

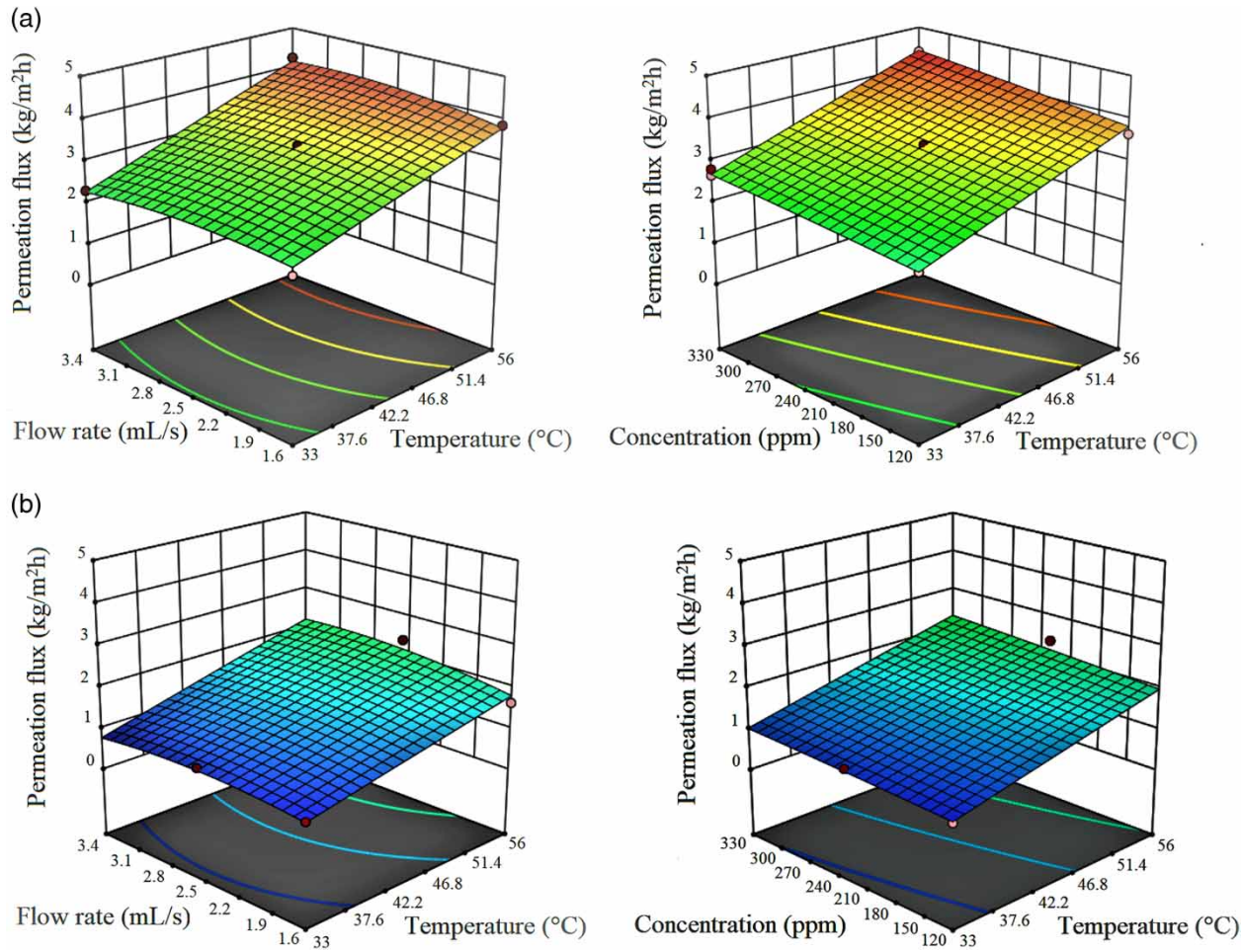

Figure 4 | Response surface plots of permeation flux in (a) 3 mm and (b) 5 mm air gaps.

there is an interaction effect between temperature and air gap width on the permeation flux, i.e., the sensitivity of the permeate flux to temperature is decreased by increasing the air gap width from 3 to 5 mm. This can be associated with the effect of increased mass transfer resistance at a higher stagnant air thickness.

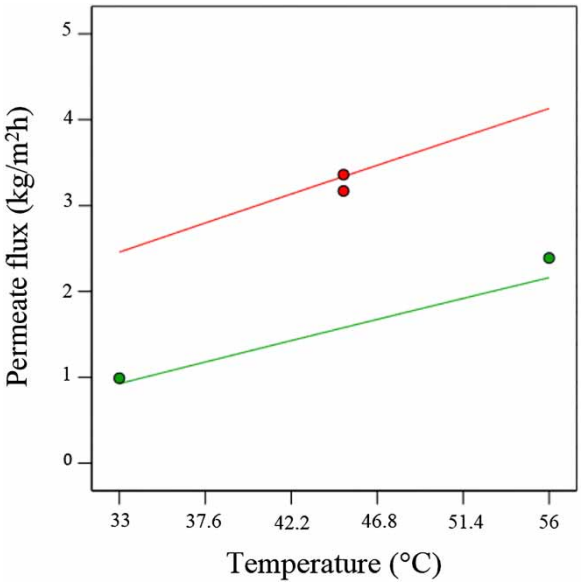

Figure 5 | Interaction plot for effect of temperature and air gap width on permeate flux.

Effects of operating parameters on separation factor

Figure 6 shows the perturbation plots for the separation factors. The curvature trend of separation factors vs. temperature in the figure demonstrates its rapid response to this factor (see Equation (5)). Increasing the feed temperature results in a slight increase in the separation factor followed by a steep decline. An increase in the feed flow rate leads to an increase in the separation factor up to a maximum value where it remains almost constant by further increase in the concentration. On the other hand, the feed concentration represents a steady positive effect on the response in the design space.

The effects of operating parameters on the separation factor of benzene are presented in Figure 7 for both 3 and 5 mm air gaps. The plots imply that temperature has a greater effect on separation factor compared to the flow rate, and increase of both variables leads to an enhancement in the separation factor. The separation factor was maximum in the mid range of the feed temperature due to the quadratic effect of the feed temperature. The diffusion coefficient for the benzene–water system in the liquid and gas phases has an increasing trend by temperature that results in an increase in the mass transfer coefficient and therefore an increase of benzene content in the permeate. However, beyond the optimum feed temperature, the thermodynamic

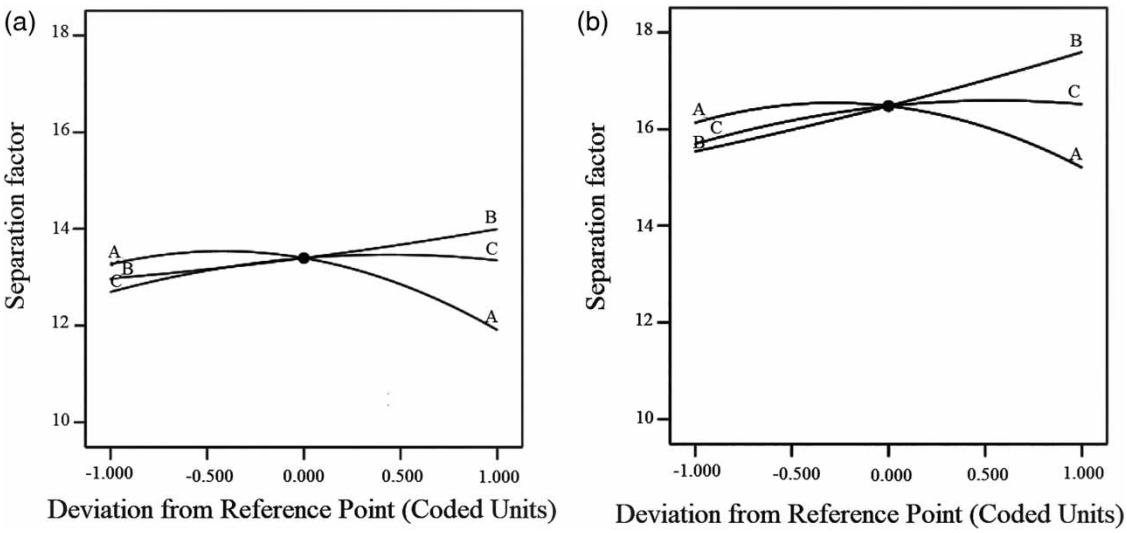

Figure 6 | Perturbation plots for separation factor in (a) $\delta = 3$ mm and (b) $\delta = 5$ mm ((A) temperature, (B) concentration, and (C) feed flow rate).

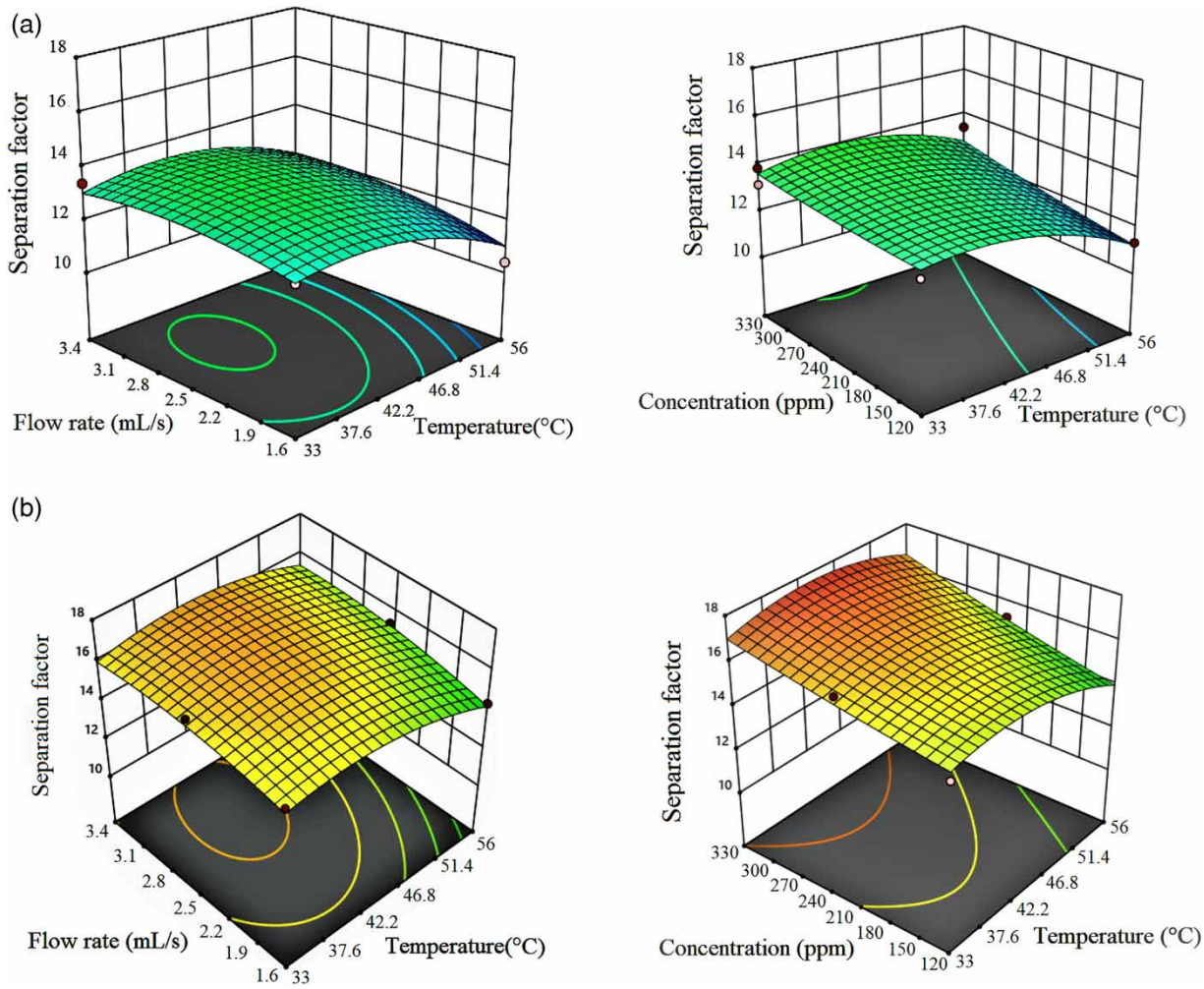

Figure 7 | Response surface plots of benzene separation factors in (a) 3 mm and (b) 5 mm air gaps.

effect will be more prominent leading to a decrease in the benzene/water vapor pressure ratio and a drop of separation factor. Adiche & Sundmacher (2010) and Banat *et al.* (1999a) reported similar trends for AGMD in separations of methanol–water and dilute ethanol–water mixtures, respectively. The observed enhancement in separation factor by feed flow rate can be attributed to increase in the mass transfer coefficient through reduction of concentration polarization at the feed/membrane interface.

As discussed in the previous section, increasing the volatile concentration in the feed leads to an increase in its vapor pressure based on Henry's law followed by a higher partial pressure difference across the membrane and therefore a higher separation factor.

The effect of air gap width on selectivity for removal of propionic acid from water was reported to be insignificant (Banat *et al.* 1999a). In addition, a well-mixed model for dilute ethanol/water mixtures did not show any notable variation in selectivity over the air gap width of 1–10 mm. However, an increase in the selectivity with the air gap width was observed, which was attributed to the Fickian mathematical model including temperature and concentration polarization effects (Banat *et al.* 1999b). A similar trend is observed in the present study, i.e., the separation factor increases with the increase of air gap width. This may be attributed to the effect of reduced permeation flux on temperature and concentration polarization (Khayet & Matsuura 2011). In addition, the reduced

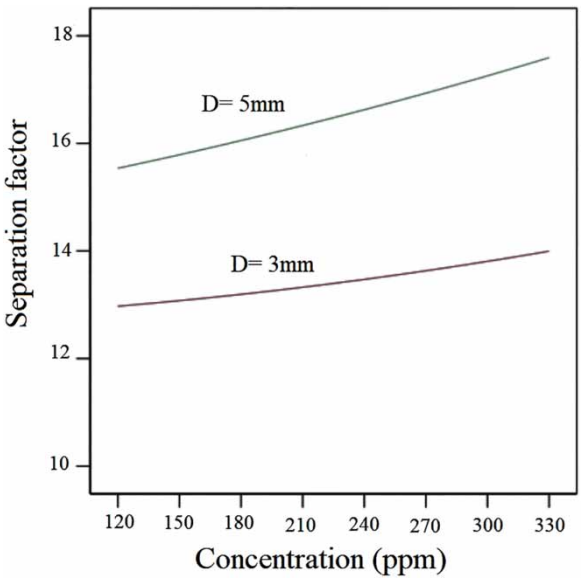

Figure 8 | Interaction plot for effect of concentration and air gap width on separation factor.

permeation flux at greater air gap thickness can affect the concentration impact on the separation factor, i.e., the separation factor increases more rapidly at higher air gap width by increasing the feed concentration, as shown in Figure 8.

Optimization and validation

The optimization tool of Design-Expert® 7.0.1 is employed to determine the optimum conditions for the AGMD performance. Since the purpose is to separate the volatile compound, the separation factor is considered as the objective function. Optimization of multiple responses takes place through a desirability function that takes values between 0 and 1 ranging from an undesirable response to a completely desirable value (Vera Candioti *et al.* 2014). To achieve the optimum conditions, all factors were selected 'within the range' while the responses, i.e., separation factor and overall permeation flux, were defined as maximum and in range, respectively.

The optimum values of process variables and related responses are represented in Table 4. The values of desirability function as a measure of optimum experimental conditions to maximize the separation factor of benzene for the reported data in Table 4 are 1 and 0.53 for air gap widths of 5 and 3 mm, respectively. This indicates that the higher air gap thickness is more acceptable. Verification experiments were performed to confirm the developed model by D-optimal design method using the suggested optimum conditions. The results given in Table 4 show good agreement with the experimental data.

Table 4 | Predicted and experimental results of permeation flux and separation factor at optimum suggested conditions

	Optimum conditions			Permeate flux (kg/m² h)		Separation factor (–)	
Air gap, δ (mm)	T (°C)	C_0 (ppm)	F_f (mL/s)	Pred.	Exp .	Pred.	Exp.
5	43	330	2.9	1.66	1.45	17.9	17.4
3	40.9	330	2.8	3.25	3.11	14.4	14.1

CONCLUSION

The AGMD performances of PTFE membranes were investigated for separation of dilute benzene from aqueous streams applying the RSM and D-optimal design. Two regression models were developed and validated statistically for permeation flux and separation factor. The effects of the feed temperature, benzene concentration, feed flow rate, air gap width, and their binary interactions on the process responses were studied. Some of the principal conclusions are as follows:

- RSM can be successfully applied for proper prediction of the MD performance including the effects of main factors and their binary interactions.
- The highest positive effect on permeation flux was attributed to the feed temperature where an increase from 35 to 65 °C would increase the permeation flux nearly two to three times. The feed concentration and flow rate had smaller positive effects.
- It was observed that temperature and air gap width are involved in an interaction effect on permeation flux. Moreover, a small interaction effect of concentration and air gap width on the separation factor was detected.

- The air gap width affects both permeation flux and separation factor, i.e., by reducing the air gap thickness, the flux increased because of reducing mass transfer resistance in the gap, and the separation factor decreases due to the effect of reduced permeation flux on temperature and concentration polarizations.
- The optimum AGMD conditions were determined at about feed inlet temperature of 43 °C, concentration of 330 ppm, and flow rate of 2.9 mL/s at 5 mm air gap thickness.

REFERENCES

Adiche, C. & Sundmacher, K. 2010 Experimental investigation on a membrane distillation based micro-separator. *Chem. Eng. Process.* **49** (4), 425–434. https://doi.org/10.1016/j.cep.2010.02.009.

AlHathal Al-Anezi, A., Sharif, A. O., Sanduk, M. I. & Khan, A. R. 2013 Potential of membrane distillation – a comprehensive review. *Int. J. Water* **7**, 317–346. https://doi.org/10.1504/IJW.2013.056674

Alklaibi, A. & Lior, N. 2005 Transport analysis of air-gap membrane distillation. *J. Membr. Sci.* **255** (1–2), 239–253. https://doi.org/10.1016/j.memsci.2005.01.038.

Alkhudhiri, A., Darwish, N. & Hilal, N. 2013 Produced water treatment: application of air gap membrane distillation. *Desalination* **309**, 46–51. https://doi.org/10.1016/j.desal.2012.09.017.

Alobaidani, S., Curcio, E., Macedonio, F., Diprofio, G., Alhinai, H. & Drioli, E. 2008 Potential of membrane distillation in seawater desalination: thermal efficiency, sensitivity study and cost estimation. *J. Membr. Sci.* **323** (1), 85–98. https://doi.org/10.1016/j.memsci.2008.06.006.

Banat, F. A., Abu Al-Rub, F., Jumah, R. & Al-Shannag, M. 1999a Application of Stefan-Maxwell approach to azeotropic separation by membrane distillation. *Chem. Eng. J.* **73** (1), 71–75. https://doi.org/10.1016/S1385-8947(99)00016-9.

Banat, F. A., Abu Al-Rub, F. & Shannag, M. 1999b Modeling of dilute ethanol–water mixture separation by membrane distillation. *Sep. Purif. Technol.* **16** (2), 119–131. https://doi.org/10.1016/S1383-5866(98)00117-8.

Bandini, S. & Sarti, G. C. 2002 Concentration of must through vacuum membrane distillation. *Desalination* **149** (1–3), 253–259. https://doi.org/10.1016/S0011-9164(02)00776-2.

Bui, V. A., Nguyen, M. H. & Muller, J. 2007 The energy challenge of direct contact membrane distillation in low temperature concentration. *Asia-Pac. J. Chem. Eng.* **2** (5), 400–406. https://doi.org/10.1002/apj.

Camacho, L., Dumée, L., Zhang, J., Li, J., Duke, M., Gomez, J. & Gray, S. 2013 Advances in membrane distillation for water desalination and purification applications. *Water* **5** (1), 94–196. https://doi.org/10.3390/w5010094.

Carlsson, L. 1983 The new generation in sea water desalination SU membrane distillation system. *Desalination* **45** (1–3), 221–222. https://doi.org/10.1016/0011-9164(83)87030-1.

Cojocaru, C. & Zakrzewska-Trznadel, G. 2007 Response surface modeling and optimization of copper removal from aqua solutions using polymer assisted ultrafiltration. *J. Membr. Sci.* **298** (1–2), 56–70. https://doi.org/10.1016/j.memsci.2007.04.001.

Couffin, N., Cabassud, C. & Lahoussine-Turcaud, V. 1998 A new process to remove halogenated VOCs for drinking water production: vacuum membrane distillation. *Desalination* **117** (1–3), 233–245. https://doi.org/10.1016/S0011-9164(98)00103-9.

Gryta, M., Tomaszewska, M. & Karakulski, K. 2006 Wastewater treatment by membrane distillation. *Desalination* **198** (1–3), 67–73. https://doi.org/10.1016/j.desal.2006.09.010.

He, K., Hwang, H. J. & Moon, I. S. 2011 Air gap membrane distillation on the different types of membrane. *Korean J. Chem. Eng.* **28** (3), 770–777. https://doi.org/10.1007/s11814-010-0415-0.

Hou, D., Wang, J., Sun, X., Ji, Z. & Luan, Z. 2012 Preparation and properties of PVDF composite hollow fiber membranes for desalination through direct contact membrane distillation. *J. Membr. Sci.* **405–406**, 185–200. https://doi.org/10.1016/j.memsci.2012.03.008.

Hwang, L. L., Tseng, H. H. & Chen, J. C. 2011 Fabrication of polyphenylsulfone/polyetherimide blend membranes for ultrafiltration applications: the effects of blending ratio on membrane properties and humic acid removal performance. *J. Membr. Sci.* **384** (1–2), 72–81. https://doi.org/10.1016/j.memsci.2011.09.005.

Khayet, M. & Cojocaru, C. 2012 Artificial neural network modeling and optimization of desalination by air gap membrane distillation. *Sep. Purif. Technol.* **86**, 171–182. https://doi.org/10.1016/j.seppur.2011.11.001.

Khayet, M. & Matsuura, T. 2011 *Membrane Distillation Principles and Applications Chemistry & Biology*. Elsevier B.V., Oxford, UK.

Khayet, M., Cojocaru, C. & García-Payo, C. 2007 Application of response surface methodology and experimental design in direct contact membrane distillation. *Ind. Eng. Chem. Res.* **46** (17), 5673–5685. https://doi.org/10.1021/ie070446p.

Khayet, M., Cojocaru, C. & Garcia-Payo, M. C. 2010a Experimental design and optimization of asymmetric flat-sheet membranes prepared for direct contact membrane distillation. *J. Membr. Sci.* **351**, 234–245. https://doi.org/10.1016/j.memsci.2010.01.057.

Khayet, M., Seman, M. N. A. & Hilal, N. 2010b Response surface modeling and optimization of composite nanofiltration modified membranes. *J. Membr. Sci.* **349** (1–2), 113–122. https://doi.org/10.1016/j.memsci.2009.11.031.

Lazic, Z. R. 2004 *Design of Experiments in Chemical Engineering*. Wiley-VCH Verlag GmbH & Co. kGaA, Weinheim, Germany.

Matheswaran, M., Kwon, T. O., Woo Kim, J. & Shik Moon, I. 2007 Factors affecting flux and water separation performance in air gap membrane distillation. *J. Ind. Eng. Chem.* **13** (6), 965–970. http://www.researchgate.net/publication/228489517_Factors_affecting_flux_and_water_separation_performance_in_air_gap_membrane_distillation/file/d912f507f8010d67e3.pdf.

Montgomery, D. C. 2001 *Design and Analysis of Experiments*, 5th edn. John Wiley & Sons, New York, USA.

Pangarkar, B. L. & Deshmukh, S. K. 2015 Theoretical and experimental analysis of multi-effect air gap membrane distillation process (ME-AGMD). *J. Environ. Chem. Eng.* **3** (3), 2127–2135. https://doi.org/10.1016/j.jece.2015.07.017.

Razmjou, A., Arifin, E., Dong, G., Mansouri, J. & Chen, V. 2012 Superhydrophobic modification of TiO2 nanocomposite PVDF membranes for applications in membrane distillation. *J. Membr. Sci.* **415–416**, 850–863. https://doi.org/10.1016/j.memsci.2012.06.004.

Summers, E. K. & Lienhard, J. H. 2013 Experimental study of thermal performance in air gap membrane distillation systems, including the direct solar heating of membranes. *Desalination* **330**, 100–111. https://doi.org/10.1016/j.desal.2013.09.023.

Vera Candioti, L., De Zan, M. M., Cámara, M. S. & Goicoechea, H. C. 2014 Experimental design and multiple response optimization. Using the desirability function in analytical methods development. *Talanta* **124**, 123–138. https://doi.org/10.1016/j.talanta.2014.01.034.

Xie, Z., Duong, T., Hoang, M., Nguyen, C. & Bolto, B. 2009 Ammonia removal by sweep gas membrane distillation. *Water Res.* **43** (6), 1693–1699. https://doi.org/10.1016/j.watres.2008.12.052.

Zolotarev, P. P., Ugrozov, V. V., Volkina, I. B. & Nikulin, V. M. 1994 Treatment of waste water for removing heavy metals by membrane distillation. *J. Hazard. Mater.* **37** (1), 77–82. https://doi.org/10.1016/0304-3894(94)85035-6.

First received 26 May 2018; accepted in revised form 1 February 2019. Available online 4 March 2019